Supporting Information Table 1. Scalar and dipolar $H_{5'}$-$H_{5''}$ couplings (in Hz) of a 24-nucleotide RNA structure, derived from helix-35 of E. coli 23S ribosomal RNA (nucleotides 737-760), and modified to contain pseudo-uridine at position 746. Values measured for H5' and H5" are listed separately. G737 is not ^{13}C-enriched and therefore not observed.

Nucleotide	$^{1}J_{H5'H5''}$	$(^{1}J+^{1}D)_{H5'H5''}$	$^{1}D_{H5'H5''}$
G_{738}	-9.2	-22.8	-13.7
G_{738}	-10.3	-21.2	-10.9
G_{739}	-11.4	-18.4	-6.9
C_{740}	-9.1	-24.2	-15.1
C_{740}	-9.9	-24.3	-14.4
U_{741}	-9.8	-22.0	-12.2
A_{742}	-9.4	-31.7	-22.2
A_{742}	-9.6	-30.3	-20.7
A_{743}	-9.0	-37.0	-28.0
U_{744}	-9.6	-39.7	-30.2
U_{744}	-10.1	-39.6	-29.5
G_{745}	-9.3	-40.5	-31.2
Ψ_{746}	-9.0	-36.0	-27.0
Ψ_{746}	-8.9	-35.2	-26.3
U_{747}	-11.1	-31.4	-20.3
U_{747}	-10.7	-34.6	-24.0
G_{748}	-10.7	-21.6	-10.8
G_{748}	-10.3	-20.5	-10.2
A_{749}	-12.5	-17.1	-4.6
A_{749}	-11.9	-18.0	-6.1
A_{750}	-11.9	-14.1	-2.2
A_{750}	-11.4	-13.2	-1.8
A_{751}	-11.4	-19.3	-7.8
A_{751}	-10.5	-19.9	-9.5
A_{752}	-11.2	-17.5	-6.3
A_{752}	-11.2	-17.1	-5.9
A_{753}	-11.3	-18.3	-6.9
A_{753}	-10.1	-19.7	-9.7
U_{754}	-11.9	-23.9	-12.0
U_{755}	-10.2	-39.1	-28.9
A_{756}	-9.6	-40.7	-31.2
A_{756}	-9.3	-38.1	-28.9
G_{757}	-8.5	-40.0	-31.5
C_{758}	-9.0	-40.7	-31.7
C_{759}	-10.3	-40.0	-29.8
C_{760}	-9.4	-38.0	-28.6
C_{760}	-9.3	-36.7	-27.7

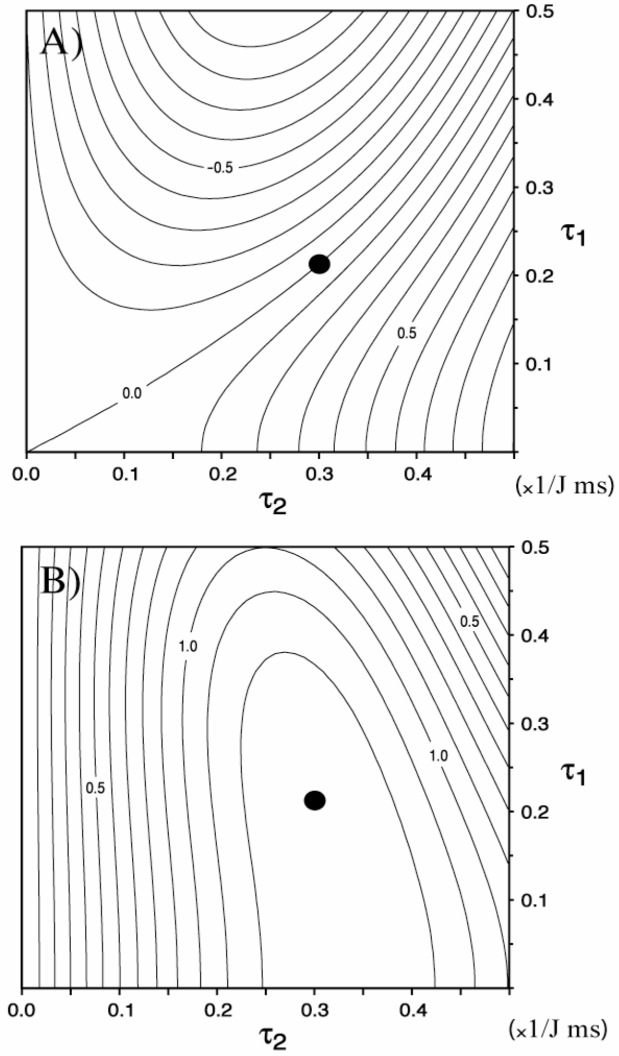

Supporting Information Figure 1. Contour plots of the intensity of the (A) downfield and (B) upfield ^{1}H-{^{1}H} doublet component as a function of τ_1 and τ_2, when using the phase cycle for selection of the upfield component. Intensities presented in the figure do not include the Boltzmann ^{13}C magnetization. The solid dot marks (τ_1, τ_2) values that yield maximum intensity (~1.3) for the selected ^{1}H-{^{1}H} doublet component. For reference, the intensity of each ^{1}H-{^{1}H} doublet component in a F_1-coupled Rance-Kay HSQC, optimized for methylene groups, equals $\sqrt{2}$.

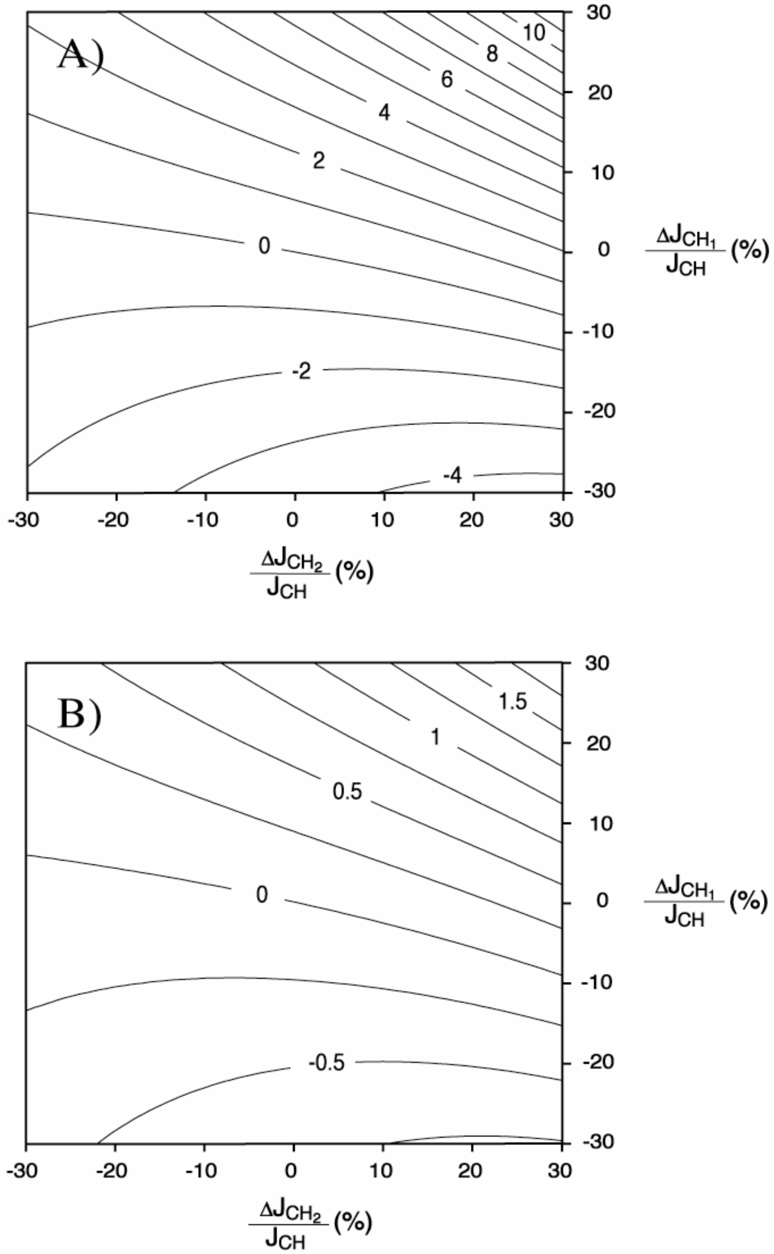

Supporting Information Figure 2. Evaluation of the ratio $(I_{H1x}-I_{H1xH2z})/(I_{H1x}+I_{H1xH2z})$ as a function of J_{CH1} and J_{CH2} mismatch. All the values reported are given in percentage.
Plot A corresponds to $(\tau_1, \tau_2) = (0.21/J_{CH1}, 0.30/J_{CH2})$,
Plot B corresponds to $(\tau_1, \tau_2) = (0.125/J_{CH1}, 0.20/J_{CH2})$

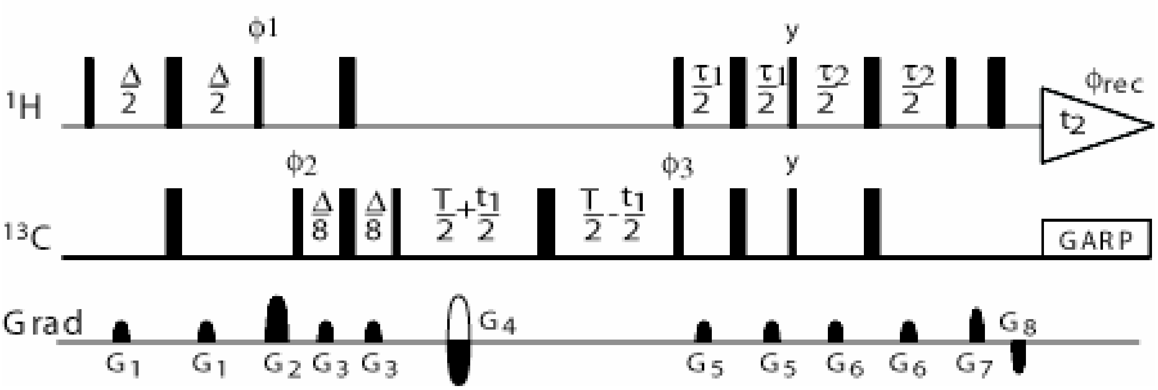

Supporting Information Figure 3. Pulse scheme of the CH_2-S^3E HSQC experiment without $90°_y$ purge pulse (applied at time point b in figure 1 of the main text). Narrow and wide bars indicate non-selective 90° and 180° pulses, respectively. Unless specified, pulse phases are *x*. Delay durations: $\Delta = 1/(2JCH) = 3.35$ ms; $\tau_1 = 2.43$ ms; $\tau_2 = 1.64$ ms. For selection of the upfield ^{13}C component: $\phi_1 = y$; $\phi_2 = (135°, -45°)$; $\phi_3 = x$; $\phi_{rec} = (x,-x)$. The experiment is recorded in the regular Rance-Kay manner: for each t_1 increment two FIDs are acquired, one with G_4 and ϕ_3 inverted, and stored separately. For selecting the ^{13}C downfield component: $\phi_1 = -y$; $\phi_2 = (225°, 45°)$; $\phi_{rec} = (x,-x)$. Field gradients are sine-bell shaped with durations $G_{1,\ldots,8}$ of 1, 2, 0.25, 2, 0.2, 0.3, 0.35, 0.153 ms, amplitudes of 10, 18, 12, 30, 10, 12, 30, 30 G/cm, and directions x, xy, y, z, xy, x, y, z, z. Single-axis *z* gradients may also be used, provided amplitude values are chosen such that accidental refocusing of unwanted pathways is avoided.

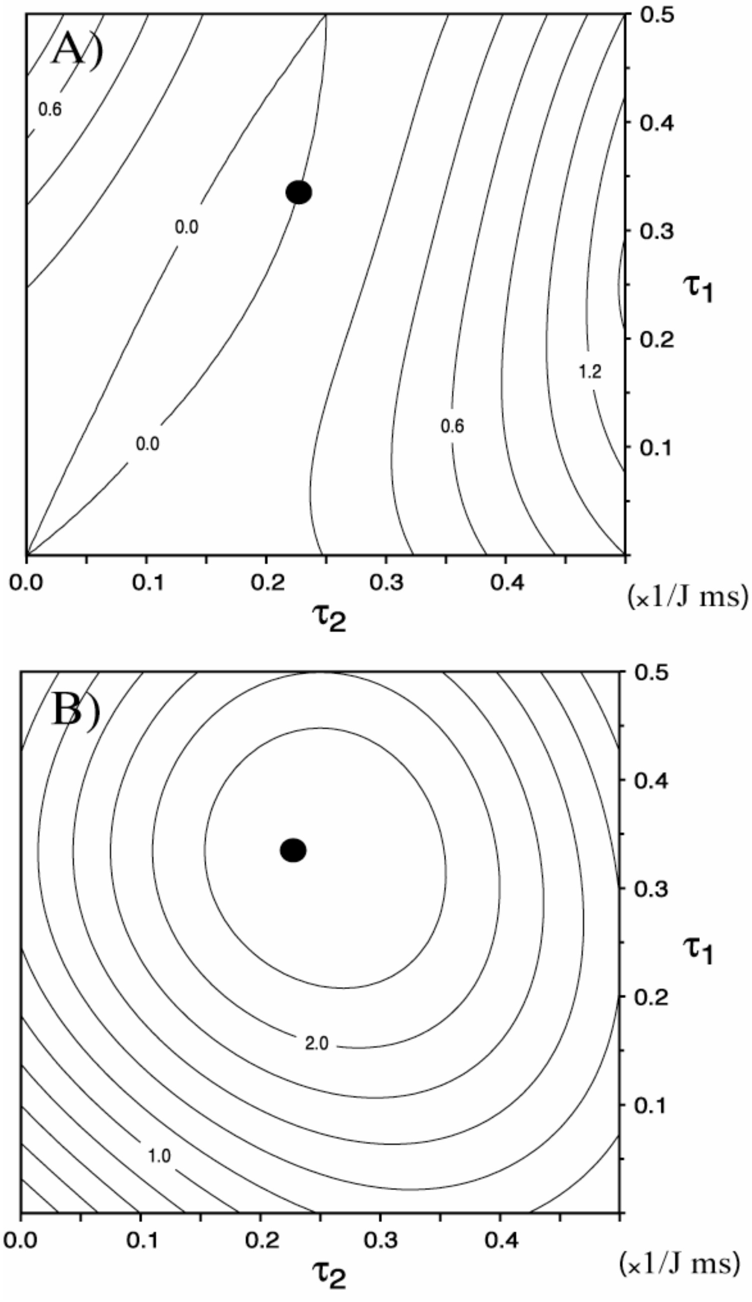

Supporting Information Figure 4. Contour plots of the intensity of the (A) downfield and (B) upfield 1H-{1H} doublet component as a function of τ_1 and τ_2, when using the sequence without purge (see Supporting Information Figure 3). Intensities presented in the figure do not include the Boltzmann ^{13}C magnetization. The solid dot marks (τ_1=0.34/J, τ_2=0.23/J) values that yield maximum intensity (~2.4) for the selected ^{1}H-{^{1}H} doublet component. For reference, the intensity of each ^{1}H-{^{1}H} doublet component in a regular F_1-coupled Rance-Kay HSQC, optimized for methylene groups, equals √2.